

# Exoplanets in Binary Star Systems

Michael Bellaver

## Abstract

As exoplanets are becoming more and more popular in the field of astronomy it is important to consider anything that might affect them. In this paper I will discuss what I have learned about exoplanets in binary star systems. I will discuss the theory and math behind how they form with two stars and how their orbits are affected by gravity from both. Then I go over a survey that was done to help understand what they look like based on previous observations, where they run tests on the samples to potentially find useful correlations. There is also a modeling paper that I read, about different types of orbits for exoplanets in binary star systems and what sort of parameters can destabilize them. Finally, I discuss the application of these first few papers on other observations that have been made with transiting data taken from the public database TESS.

## 1 Introduction

Exoplanets are planets that have been discovered in other star systems, other than our solar system. Recently they have become more popular as a new way of detecting them and confirming them has become more popular. This method I called the transit method. The way that the transit method works is that using

photometry, we measure the light coming from a star and when an exoplanet moves in front of the star the light will slightly dim for a period of that while the exoplanet is in front of the star. With enough knowledge of the host star, we can use this information to determine things such as the radius of the exoplanet.

Other forms of exoplanet detection include radial velocity, which reads the wavelength from the star and looks for instances of higher frequencies, caused by an exoplanet. Direct imaging, which is done by removing the glare from a star which reveals an exoplanet. Gravitational microlensing, which is done by measuring how the light from a distant star is bent due to the gravitational field of the exoplanet orbiting it as it passes between the star and earth. And finally, astrometry, which is done by measuring the wobble of the position of a star relative to neighbor stars.

Much like our planet and the planets in our solar system, exoplanets form through dust that is orbiting a star colliding with other dust, slowly forming a gravitational field and then causing more and more dust to collide with it until it has cleared an elliptical path around the host star which we call its orbit.

When it comes to exoplanets, their orbits and how they change around a single star is something that is quite well known now. However single star systems are not the most common type of star system. It is much more common to have a binary star system, as it is estimated that most star systems are binary star systems. This makes understanding binaries much more important for understanding the vastness of space as we know it. Thus, understanding how a binary will affect the

orbits of exoplanets in said star system is a key feature to learning more about the universe because most of all Sun-like stars have at least one planet that has formed. Ever since 2011 when Kepler-14 was the first exoplanet in a binary star system (Doyle, L. R et al 2011), the topic of exoplanets in binaries has become a very hot topic, both in the theoretical and observational communities.

In this paper I will be discussing how we have come to a deeper understanding of the structure of orbits and the effects on them due to two stars being present, I have gathered this information by going through scientific papers on the theory, math, and modeling of these exoplanets. I will further elaborate on this information presented and report ties that I have found throughout the individual papers as they may arise.

## 2 Theory & Structure

For a planet to form it must rely on the ability of particles, such as dust and planetesimals, to interact. This is easy to do around a single star due to the consistency of orbits around said star. Due to gravity from these particles, collisions occur which in turn cause the particles to grow, increasing their gravity and thus the collisions that occur.

For a binary star system this consistent orbit is changed. For two stars in a system that have similar masses and binary eccentricity,  $e_{bin}$ , orbits become unstable within a certain radius,  $a_{crit}$ , and this number is at least two times the binary separation,  $a_{bin}$ . In 1999 Matthew J. Holman and Paul A. Wiegert derived an approximation for the variable  $a_{crit}$  by simulating circumbinary particles:

$$a_{crit} \approx 1.60 + 5.10e_{bin} - 2.22e_{bin}^2 + 4.12 \frac{M_s}{M_p + M_s} - 4.27e_{bin} \frac{M_s}{M_p + M_s} \\ - 5.09 \frac{M_s^2}{(M_p + M_s)^2} + 4.61e_{bin}^2 \frac{M_s^2}{(M_p + M_s)^2}$$

Where  $M_p$  is the mass of the primary star and  $M_s$  is the mass of the secondary star.

Inside of this critical radius the particles are cleared, which creates a cavity around the binary where planets cannot form.

Outside of this critical radius planets can form stably, but only in non-Keplerian orbits (Bromley & Kenyon 2015). Due to the binary's time-varying potential these particles also experience forced motion. This forced motion prevents them from maintaining circular or eccentric orbits (Bromley & Kenyon 2015). Because of this the particles must instead create a “most circular orbit,” which is defined as having the smallest radial excursion around a center, orbiting at a constant radius,  $R_g$ , and angular speed,  $\Omega_g$ , in the plane of the binary (Lee & Peale 2006; Youdin et al. 2012). Eccentric circumbinary orbits may be composed of epicyclic motion about  $R_g$ , as in the keplerian case, superimposed of the most circular orbit (Bromley & Kenyon 2015).

## 2.1 Analytical Theory

Starting on the analytical theory of the orbits in a binary star system we must first consider the Lee-Peale-Leung analysis of the gravitational potential of the binary star system:

$$\Phi = - \frac{GM_p}{\sqrt{R^2 + z^2 + R_p^2 + 2RR_p \cos(\Delta\phi)}} - \frac{GM_s}{\sqrt{R^2 + z^2 + R_s^2 - 2RR_s \cos(\Delta\phi)}}$$

In which,  $\Delta\phi$  is the angle between the secondary and the particle that are moving around the stars in a reference frame with the center of the binary's mass is at the origin (Bromley & Kenyon 2015).  $R$  and  $z$  are radial position in the binary and the altitude above this plane respectively.

To get the equations of motion, we take the derivatives of the gravitational potential equation in the excursion coordinates  $(\delta R, \delta\phi, z)$ . Lee & Peale (2006) did this by using a forced harmonic oscillator with the frequencies  $\kappa_e$  for  $\delta R$  and  $\delta\phi$ , and  $\nu_i$  for  $z$ , and the driving frequencies  $\Omega_{bin}$  and  $\omega_{syn}$ .

$$\kappa_e^2 \equiv R_g \frac{d\Omega_g^2}{dR} + 4\Omega_g^2$$

$$\nu_i^2 \equiv \frac{1}{z} \frac{d\Phi}{dz}$$

$$\omega_{syn} = \Omega_{bin} - \Omega_g$$

$$\begin{aligned} R(t) &= R_g \left\{ 1 - e_{free} \cos(\kappa_e t + \psi_e) - \sum_{k=1}^{\infty} C_k \cos(k\omega_{syn} t) \right. \\ &\quad \left. - e_{bin} \left[ \tilde{C}_0^e \cos(\Omega_{bin} t) + \sum_{k=1}^{\infty} \tilde{C}_k^+ \cos(k\omega_{syn} t + \Omega_{bin} t) + \tilde{C}_k^- \cos(k\omega_{syn} t - \Omega_{bin} t) \right] \right\} \\ \phi(t) &= \Omega_g \left\{ t + \frac{2e_{free}}{\kappa_e} \sin(\kappa_e t + \psi_e) + \sum_{k=1}^{\infty} \frac{D_k}{k\omega_{syn}} \sin(k\omega_{syn} t) \right. \\ &\quad \left. + e_{bin} \left[ \frac{\tilde{D}_0^e}{\Omega_{bin}} \cos(\Omega_{bin} t) + \sum_{k=1}^{\infty} \frac{\tilde{D}_k^+ \sin(k\omega_{syn} t + \Omega_{bin} t)}{k\omega_{syn} + \Omega_{bin}} + \frac{\tilde{D}_k^- \sin(k\omega_{syn} t - \Omega_{bin} t)}{k\omega_{syn} - \Omega_{bin}} \right] \right\} \\ z(t) &= i R_g \cos(\nu_i t + \psi_i), \end{aligned}$$

Both sums for from  $k = 1$  to infinity and  $e_{free}$  is the free eccentricity. Every  $C$  and  $D$  is a unique coefficient for determining  $R(t)$  and  $\phi(t)$  shown below.

$$\begin{aligned}
C_k &= \frac{1}{R_g(\kappa_e^2 - k^2\omega_{\text{syn}}^2)} \left[ \frac{d\Phi_{0k}}{dR} - \frac{2\Omega_g\Phi_{0k}}{R_g\omega_{\text{syn}}} \right]_{R_g} \\
\tilde{C}_0^e &= -\frac{1}{R_g(\kappa_e^2 - \Omega_{\text{bin}}^2)} \left[ \frac{d\Phi_{00}^e}{dR} \right]_{R_g} \\
\tilde{C}_k^\pm &= \frac{1}{R_g[\kappa_e^2 - (k\omega_{\text{syn}} \pm \Omega_{\text{bin}})^2]} \left[ \pm k \frac{d\Phi_{0k}}{dR} - \frac{1}{2} \frac{d\Phi_{0k}^e}{dR} - \frac{k\Omega_g(\pm 2k\Phi_{0k} - \Phi_{0k}^e)}{R(k\omega_{\text{syn}} \pm \Omega_{\text{bin}})} \right]_{R_g} \\
D_k &= 2C_k + \left[ \frac{\Phi_{0k}}{R_g^2\Omega_g\omega_{\text{syn}}} \right]_{R_g}, \\
\tilde{D}_0^e &= 2\tilde{C}_0^e \\
\tilde{D}_k^\pm &= 2\tilde{C}_k^\pm + \left[ \frac{k(\pm 2k\Phi_{0k} - \Phi_{0k}^e)}{2R_g^2\Omega_g(k\omega_{\text{syn}} \pm \Omega_{\text{bin}})} \right]_{R_g}
\end{aligned}$$

From these solutions by Leung & Lee (2013), we can see two independent modes.

The first mode being forced motion which is determined using the characteristics of the binary and the orbital distance of the particles from the center of mass. The second is free motion which is affected by the eccentricity and inclinations of the orbits (Bromley & Kenyon 2015).

When the eccentricity of the binary becomes big, we must update the equation for  $R(t)$  to account for the forced eccentricity.

$$R(t) = R_g[1 - e_{\text{free}}\cos(\kappa_e t + \psi_e) - e_{\text{force}}\cos(\Omega_g t) + \dots]$$

An important thing to know about the forced eccentric orbit is that it does not precess. However, all the other parts of the forced motion are synchronous with the binary stars.

When it comes to free motion, free eccentricity and inclination are both related to the precession. This is because the time-averaged potential around a binary does not fall off as  $1/R$  (Heppenheimer 1978; Murray & Dermott 1999; Lee & Peale 2006).

The Precession rates of the periastron and ascending nodes are:

$$\dot{\omega} = \Omega_g - \kappa_e \approx \frac{3}{4} \frac{a_{bin}^2}{R_g^2} \frac{\mu}{M} \sqrt{GM/R_g^3}$$

$$\dot{\Omega}_{node} = \Omega_g - v_i \approx -\frac{3}{4} \frac{a_{bin}^2}{R_g^2} \frac{\mu}{M} \sqrt{GM/R_g^3}$$

This shows them to be approximately equal and opposite (Bromley & Kenyon 2015).

### 3 Architecture

After going through the theory of how a Binary star system is formed and behaves, we then go to observational data to test the theories that have been developed. In

System	$t_0$ (MJD)	$\Delta t$ (yr)	$\rho_0$ (mas)	$\theta_0$ ( $^\circ$ )	$\dot{\rho}$ (mas yr $^{-1}$ )	$\dot{\theta}\rho_0$ (mas yr $^{-1}$ )
KOI-0001AB	56956	3.95	1109.37 $\pm$ 0.27	136.368 $\pm$ 0.012	1.90 $\pm$ 0.16	0.15 $\pm$ 0.14
KOI-0042AB	56927	4.11	1665.8 $\pm$ 0.4	35.581 $\pm$ 0.012	-0.66 $\pm$ 0.24	0.52 $\pm$ 0.20
KOI-0112AB	57405	2.93	100.7 $\pm$ 0.5	114.13 $\pm$ 0.21	0.0 $\pm$ 0.4	-1.7 $\pm$ 0.3
KOI-0214AB	57053	0.94	68.0 $\pm$ 1.6	195.4 $\pm$ 1.5	-6 $\pm$ 3	-2 $\pm$ 4
KOI-0227AB	56985	2.96	299.73 $\pm$ 0.11	69.002 $\pm$ 0.019	0.01 $\pm$ 0.09	1.04 $\pm$ 0.07
KOI-0249AB	56688	2.94	4333.0 $\pm$ 1.3	28.078 $\pm$ 0.017	0.5 $\pm$ 0.9	-0.4 $\pm$ 0.8
KOI-0270AB	57301	1.96	168.31 $\pm$ 0.10	64.344 $\pm$ 0.026	2.60 $\pm$ 0.12	0.38 $\pm$ 0.11
KOI-0291AB*	57349	2.90	65.69 $\pm$ 0.18	316.2 $\pm$ 0.4	-0.47 $\pm$ 0.16	-0.3 $\pm$ 0.3
KOI-0588AB	56600	2.95	280.31 $\pm$ 0.10	276.327 $\pm$ 0.015	0.44 $\pm$ 0.07	-0.93 $\pm$ 0.06
KOI-0854AB	57071	3.18	17.7 $\pm$ 0.6	222.1 $\pm$ 2.7	1.0 $\pm$ 0.4	2.6 $\pm$ 0.5
KOI-0975AB	57254	2.28	776.31 $\pm$ 0.30	129.474 $\pm$ 0.020	3.3 $\pm$ 0.3	1.21 $\pm$ 0.29
KOI-1422AB	56863	2.03	214.16 $\pm$ 0.11	216.927 $\pm$ 0.023	-0.76 $\pm$ 0.14	-0.33 $\pm$ 0.10
KOI-1613AB	57225	4.90	207.60 $\pm$ 0.05	184.519 $\pm$ 0.016	-1.47 $\pm$ 0.04	0.01 $\pm$ 0.04
KOI-1615AB	56906	4.21	24.8 $\pm$ 0.8	135.6 $\pm$ 1.5	-3.5 $\pm$ 0.4	2.7 $\pm$ 0.4
KOI-1619AB	57015	4.34	2068.8 $\pm$ 0.6	226.605 $\pm$ 0.012	1.0 $\pm$ 0.3	-0.66 $\pm$ 0.23
KOI-1681AB	56863	2.03	148.61 $\pm$ 0.16	141.19 $\pm$ 0.03	-1.83 $\pm$ 0.22	-0.13 $\pm$ 0.09
KOI-1725AB	56974	0.82	4053.4 $\pm$ 1.2	98.567 $\pm$ 0.013	-7 $\pm$ 4	-2.5 $\pm$ 2.5
KOI-1835AB	57175	4.88	53.9 $\pm$ 0.4	355.49 $\pm$ 0.28	-1.28 $\pm$ 0.29	0.45 $\pm$ 0.18
KOI-1841AB	57048	4.90	309.46 $\pm$ 0.12	74.097 $\pm$ 0.020	0.90 $\pm$ 0.06	-0.24 $\pm$ 0.05
KOI-1961AB*	57432	2.92	38.51 $\pm$ 0.10	262.3 $\pm$ 0.7	2.59 $\pm$ 0.09	2.0 $\pm$ 0.4
KOI-1962AB	57079	3.92	123.18 $\pm$ 0.21	114.09 $\pm$ 0.05	2.06 $\pm$ 0.16	0.30 $\pm$ 0.09
KOI-1964AB	57064	4.02	386.18 $\pm$ 0.09	1.063 $\pm$ 0.012	-3.23 $\pm$ 0.06	-1.82 $\pm$ 0.05
KOI-1977AB	56796	3.92	81.08 $\pm$ 0.15	77.03 $\pm$ 0.25	-1.45 $\pm$ 0.10	-1.2 $\pm$ 0.8
KOI-2005AB*	57246	3.93	20.26 $\pm$ 0.30	237 $\pm$ 4	0.89 $\pm$ 0.27	-1.1 $\pm$ 0.9
KOI-2031AB*	57132	3.93	56.0 $\pm$ 0.6	246.6 $\pm$ 1.4	-0.3 $\pm$ 0.4	-0.1 $\pm$ 0.9
KOI-2059AB	56511	1.96	385.44 $\pm$ 0.21	289.573 $\pm$ 0.020	1.17 $\pm$ 0.21	-1.21 $\pm$ 0.14
KOI-2124AB*	56985	4.88	56.5 $\pm$ 1.1	53.54 $\pm$ 0.15	3.1 $\pm$ 0.5	0.04 $\pm$ 0.07
KOI-2179AB	56861	2.02	133.6 $\pm$ 0.4	356.09 $\pm$ 0.10	-1.0 $\pm$ 0.4	-0.10 $\pm$ 0.22
KOI-2295AB	56966	3.94	2188.1 $\pm$ 1.0	78.563 $\pm$ 0.014	-0.3 $\pm$ 0.7	1.5 $\pm$ 0.3
KOI-2418AB	57345	2.94	103.7 $\pm$ 0.6	2.1 $\pm$ 0.3	-1.5 $\pm$ 0.5	0.1 $\pm$ 0.5
KOI-2542AB	56863	2.02	764.11 $\pm$ 0.21	28.674 $\pm$ 0.013	-0.26 $\pm$ 0.26	-0.42 $\pm$ 0.21
KOI-2672AB	56869	1.97	640.09 $\pm$ 0.23	306.502 $\pm$ 0.020	-2.23 $\pm$ 0.25	0.80 $\pm$ 0.24
KOI-2705AB	57265	2.28	1888.4 $\pm$ 0.5	303.900 $\pm$ 0.017	-0.8 $\pm$ 0.5	-0.8 $\pm$ 0.7
KOI-2733AB	57266	2.30	105.62 $\pm$ 0.18	294.61 $\pm$ 0.13	-2.47 $\pm$ 0.22	1.05 $\pm$ 0.26
KOI-2790AB	57405	2.93	253.25 $\pm$ 0.09	135.017 $\pm$ 0.023	-0.63 $\pm$ 0.09	0.36 $\pm$ 0.10
KOI-3158AB	57325	0.99	1841.9 $\pm$ 0.4	252.834 $\pm$ 0.013	-0.6 $\pm$ 1.0	-0.1 $\pm$ 0.9
KOI-3255AB	57266	2.30	181.21 $\pm$ 0.07	336.006 $\pm$ 0.027	-0.42 $\pm$ 0.09	-0.15 $\pm$ 0.10
KOI-3284AB	57046	0.98	438.69 $\pm$ 0.17	192.802 $\pm$ 0.020	-0.5 $\pm$ 0.3	-0.2 $\pm$ 0.3
KOI-3444AB	57222	1.84	1085.33 $\pm$ 0.27	9.718 $\pm$ 0.014	2.4 $\pm$ 0.4	-0.6 $\pm$ 0.3
KOI-3892AB	57053	0.94	120.8 $\pm$ 1.6	341.8 $\pm$ 0.8	8 $\pm$ 3	10 $\pm$ 3
KOI-3991AB	57267	2.29	201.17 $\pm$ 0.24	111.60 $\pm$ 0.03	-1.63 $\pm$ 0.21	0.63 $\pm$ 0.23
KOI-4032AB	56690	0.98	126.2 $\pm$ 0.7	30.6 $\pm$ 0.3	1.8 $\pm$ 1.4	-0.2 $\pm$ 1.5
KOI-4097AB	57209	3.91	176.8 $\pm$ 0.6	17.84 $\pm$ 0.14	-1.5 $\pm$ 0.3	5.33 $\pm$ 0.24
KOI-4184AB*	57227	3.91	206.47 $\pm$ 0.05	223.25 $\pm$ 0.05	0.30 $\pm$ 0.03	-0.23 $\pm$ 0.13
KOI-4252AB	57488	2.88	48.11 $\pm$ 0.15	341.29 $\pm$ 0.15	3.05 $\pm$ 0.10	-3.53 $\pm$ 0.08

Table 1. Linear fits to the relative astrometry time series measurements of planet hosting binaries.

the scientific paper “*Orbital Architecture of Planet-Hosting Binaries II. Low Mutual Inclinations Between Planetary and Stellar Orbits*,” Dupuy and additional contributors go over 45 binary star systems that host Kepler planet candidates. This study was done over a course of 5 years and the results bring a very good opportunity to bring a better understanding of exoplanets in binary star systems. The sample shown in *table 1* is a list of the binary systems used in the study. It is expected that the binaries in this sample should generally display orbital motion that is indistinguishable from linear motion within certain astrometric errors (Dupuy et al. 2022). Within the sample the two smallest estimated orbital periods are 11 and 16 years and in the time of this survey there was no evidence that of nonlinear motion that appeared, which in turn provides some grounds for the assumption of the orbital motion not being distinguishable from the orbital motion. To have done this they had to fit each set of separations and PAs as a function of time, this would give, in return, an instant measurement of the orbital motion at the mean epoch of the input data (Dupuy et al. 2022). Table 1 also includes the information that resulted from fitting.

Since most of the binaries in this survey have not been observationally confirmed as bound pairs, they had to use the equation:

$$B \equiv \frac{1}{8\pi^2} \left( \frac{d}{pc} \right)^3 \left( \frac{\sqrt{\dot{\rho}^2 + \dot{\theta}^2}}{arcsec/yr} \right)^2 \left( \frac{\rho_0}{arcsec} \right) \left( \frac{M_{tot}}{M_{\odot}} \right)^{-1}$$

This equation depends on the distance (d), total angular velocity, angular separation, and the total mass of the system ( $M_{tot}$ ). For bound companions, B needs



to be less than 1 (Dupuy et al. 2022). All but three of the systems are clearly bound, this includes KOI-0214AB, KOI-1725AB, and KOI-3892AB.

### 3.1 Testing

Dupuy decided to run three different tests to determine the most likely inclinations between the exoplanets and their hosting binary. In order to have a reasonable result one must understand that having a perfect edge on inclination is very difficult, so in the test they decided to refer to low inclinations as “aligned” and high inclinations as “misaligned” (Dupuy et al. 2022).

The first test that they decided to use was the binary variable test. This means that they are testing for a basic yes or no on whether it is aligned. The advantages to this are that it’s very simple and can be done by easy statistical tests such as the binomial theorem. They use a Monte Carlo test where the null hypothesis is set to be that binary orbital inclinations are distributed with isotropic viewing angles,  $p(i) \propto \cos(i)$  (Dupuy et al. 2022). The results of this showed that 35% of the trial had more aligned orbital arcs where  $|\dot{\rho}| > |\dot{\theta}|$ . This was an unexpected result because the isotropic viewing angle would mean that edge-on orbits should be more common.

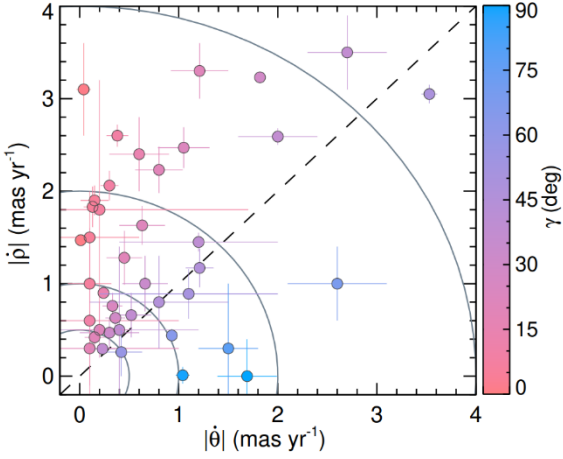


Figure 1. Amplitude of the orbital motion in the separation direction as a function of the amplitude of orbital motion in the PA direction for the sample systems. Color indicates how consistent with being edge on (red) or face on (blue) the orbital motion is.

Figure 1 shows the orbital arcs. 33 out of the 45 have more aligned orbital arcs, which is a much greater number than the result from the Monte Carlo simulation. The probability of 33 out of the 45 being more aligned is  $2e-7$  when you factor in the 35% chance of each individual happening according to the Monte Carlo simulation. With this in mind, we can

safely believe that the null hypothesis can be ruled out due to the high significance of this probability.

The second test that they employed is a mass and distance independent test. For this test they focus on the velocities in a moment. Using the velocity, we can determine the direction and speed of the exoplanets. Of the two characteristics, the direction is easy and only relies on a few parameters. However, speed is a much more difficult task in this situation. The issue that arrives with the speed of the exoplanets is: one, the speed is measured in angular units, which we must convert to a more physical understanding; two, it requires acceleration and mass to find, but as this is a mass independent test, they decided to only focus on the direction. They use the angle between the direction of orbital motion and the binary PA ( $\gamma$ ) as the mass and distance independent variable (Dupuy et al. 2022).

$$\gamma \equiv \arctan(|\dot{\theta}|, |\dot{\rho}|)$$

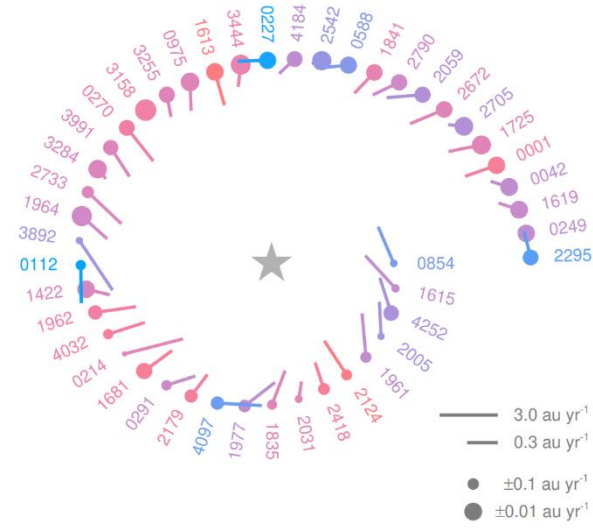


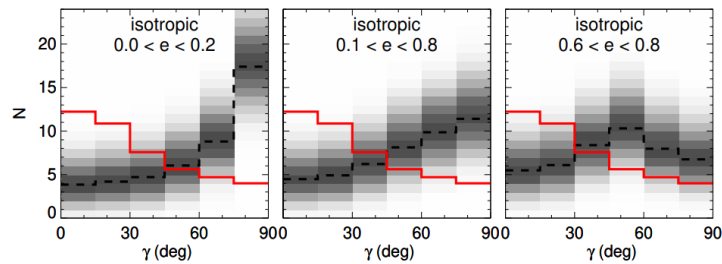
Figure 2. Pictorial representation of our orbital motion measurements. Binary companions are arranged in a spiral pattern, in order of increasing separation in AU (but not shown to scale), around a star symbol that depicts the (typically) planet-hosting primary.

Figure 2 is a representation of the orbital motion around each respective star. This shows the speed, direction, and astrometric precision as a function of separation (Dupuy et al. 2022). Figure 3 shows the  $\gamma$  for the 45 orbit arcs that were measured (Dupuy et al. 2022). The uncertainties are accounted for by using Monte Carlo testing, which focuses on the Gaussian-distributed values and

turns them into  $\gamma$  values that are not necessarily in a Gaussian distribution (Dupuy et al. 2022).

To compare the measured  $\gamma$ , they did a Monte Carlo simulation to create orbits similar to the orbits in the survey. The null hypothesis that they chose is that it

would  
field binary  
which is  
over a wide  
eccentricities (Raghavan et al. 2010).



resemble the  
population  
roughly flat  
range of

Figure 3. Histograms of simulated  $\gamma$  values for isotropic inclinations and different eccentricity distributions that range from more circular (left) to field binary-like (middle) to highly eccentric (right).

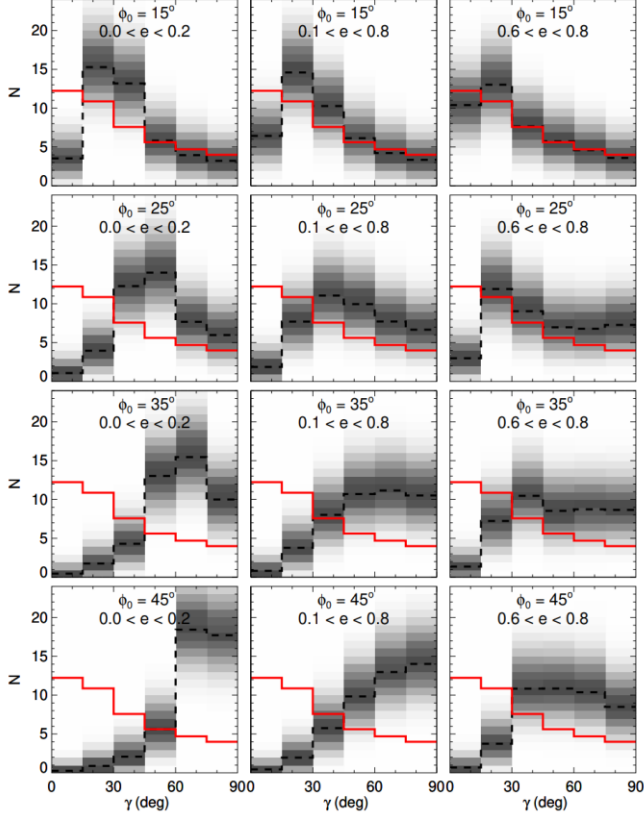


Figure 5. Histograms of simulated  $\gamma$  values, same as figure 3, except here the planet-binary mutual inclinations are misaligned by the angle plus or minus 5 degrees.

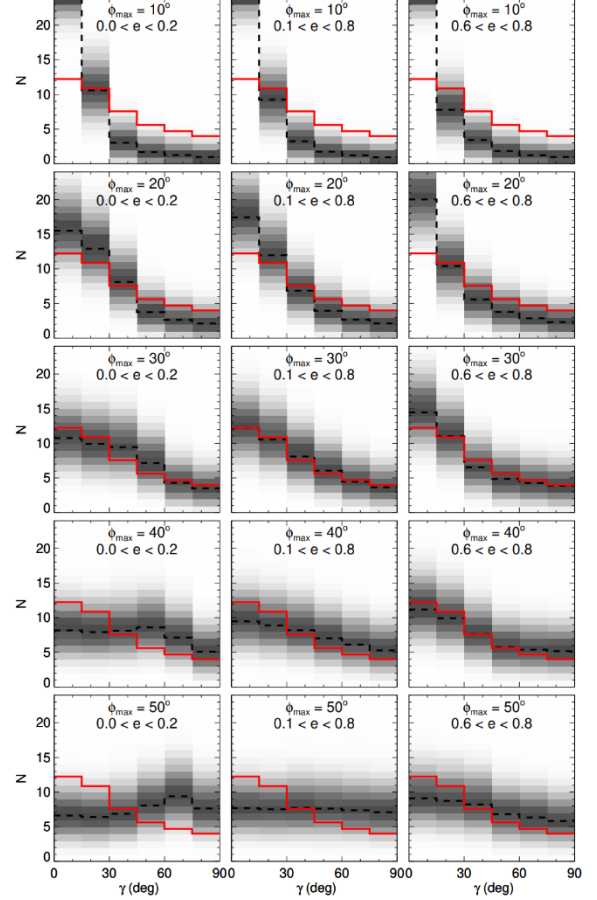


Figure 4. Histograms of simulated  $\gamma$  values, same as figure 3, except here the planet-binary mutual inclinations are uniformly distributed from perfectly aligned up to maximum misalignment of the maximum angle.

Figure 3 shows us the distribution for  $\gamma$  for

isotropic orbital inclinations, as would be expected if the transiting planet orbital plane were independent of the binary orbital plane (Dupuy et al. 2022). An interesting find in this simulation is that all the distributions have a minimum when they have low  $\gamma$ . This contradicts the distribution made by the observed data, which has its minimum at a high  $\gamma$ .

For figure 4 shows the distributions when the planet and the binary are misaligned by a specified amount. Generally, highly misaligned orbits do not provide a good match to the observed distribution, and in comparison, figure 5 which is highly aligned orbits. Neither are particularly useful as they are extremes that aren't common (Dupuy et al. 2022).

The third test that Dupuy used is the two-population test. Assuming that there could be multiple ways for formation pathways to go to produce the survey, they considered the possibility that two disparate populations could explain the observed distribution of  $\gamma$ . Ultimately the two-populations tests show that the majority of the sample must show some degree of alignment between the planet and binary orbits. If some were misaligned, then the rest would have to be even more aligned than previously shown in the single-population tests (Dupuy et al. 2022).

The results of these tests lead Dupuy and company to discover that the orbital planes of the planet-hosting binary sample are not coming from a random distribution, they only work if the mutual inclination of the stellar and planetary orbits are low. This means that the planets must orbit on a similar axis to the stars (Dupuy et al. 2022).

## 4 Modeling

In the paper “*Stability of Planetary Motion in Binary Star Systems*” R. Capuzzo-Dolcetta et al. (2020) models 3 different categories of binary systems which we classified by Dvorak in 1986. The first ones are the planet type (P-type), where the planet orbits on the exterior of both stars in the binary. The second is the satellite type (S-type), which only orbits around one of the two stars in the binary. The third type is the liberation type (L-type), these correspond to liberations around the Lagrangian equilibrium points  $L_4$  and  $L_5$ , which are stable when the stellar mass ration is less than 0.04 (Capuzzo-Dolcetta et al. 2020). However, since L-type orbits are not of concern for a binary system, they were not actually modeled in this scientific paper.

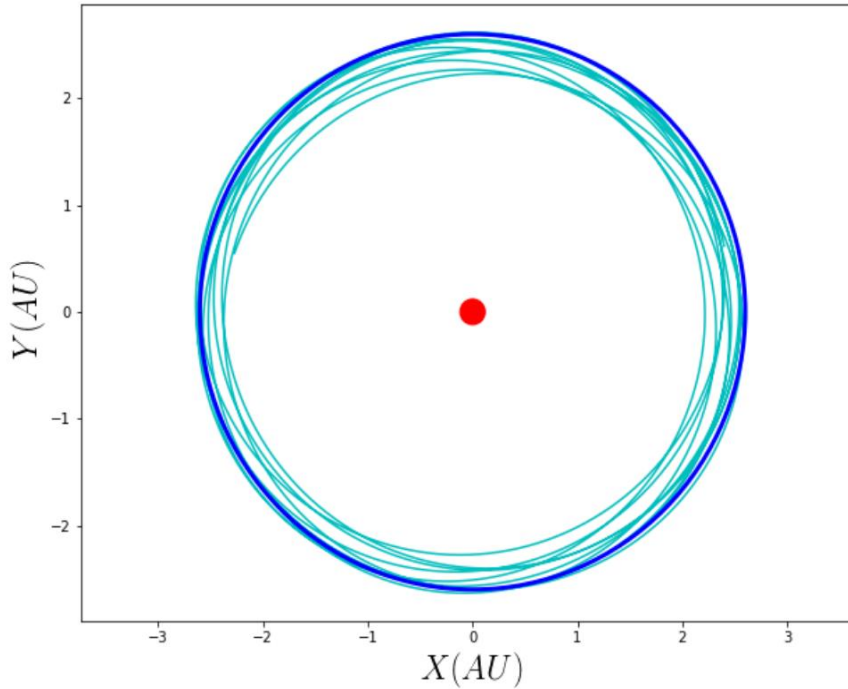
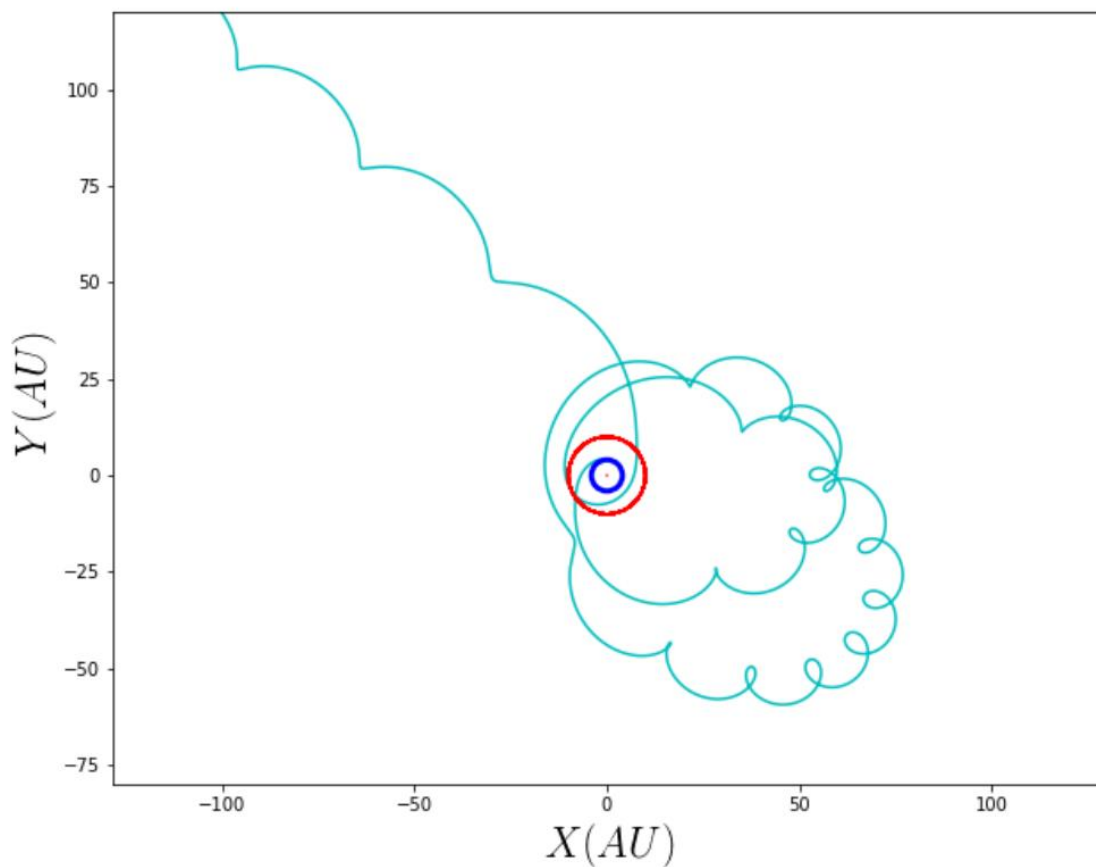


Figure 6. This is an example of a stable orbit around on of the stars in the binary. The other star in the binary is at 10 au from this star (red dot). The cyan line is the planet showing the effect of the second star and the dark blue line has no effect from the second star.

In the models they integrate the orbits while changing the initial conditions. They changed the mass ratio between the two stars, their orbital eccentricity, the initial planetary orbital radius, and the planet's mass. This created a dataset of over ten thousand orbits. To read out only the stable orbits they set a quantitative criterion based on the variation of the planet trajectory with respect to the initial one (Capuzzo-Dolcetta et al. 2020). The orbits are classified as unstable if the planet collides with one of the stars, or the planet is thrown out of the system.



*Figure 7. This is an example of the planet in the binary star system being ejected.*

Something interesting about this is that according to the theory, this cannot have formed in situ. The planet in this model would have had to move in between the stars because of the critical radius that the star creates where planets cannot for due to there not being any dust or particles to collide with.

In figure 7 we are shown a case where one of the simulations resulted in an unstable orbit and the planet was thrown out of the star system due to one of the initial parameters causing a large disturbance.

		Critical semi-major axis ( $m_p = 0, 30 M_J$ )								
		$\mu$								
$e$	$m (M_J)$	0.10	0.20	0.30	0.40	0.50	0.60	0.70	0.80	0.90
0.0	30	0.43	0.36	0.38	0.31	0.27	0.23	0.20	0.17	0.13
	0	0.45	0.38	0.37	0.30	0.26	0.23	0.20	0.16	0.13
0.1	30	0.37	0.31	0.30	0.28	0.24	0.21	0.18	0.15	0.11
	0	0.37	0.32	0.29	0.27	0.24	0.21	0.18	0.15	0.11
0.2	30	0.32	0.27	0.26	0.23	0.20	0.19	0.16	0.13	0.10
	0	0.32	0.27	0.25	0.23	0.21	0.19	0.16	0.13	0.10
0.3	30	0.26	0.24	0.21	0.19	0.18	0.16	0.14	0.12	0.09
	0	0.28	0.24	0.21	0.19	0.18	0.16	0.14	0.12	0.09
0.4	30	0.21	0.20	0.18	0.16	0.14	0.13	0.12	0.10	0.07
	0	0.23	0.20	0.18	0.16	0.14	0.13	0.11	0.10	0.07
0.5	30	0.16	0.15	0.14	0.13	0.12	0.10	0.09	0.08	0.06
	0	0.18	0.16	0.14	0.13	0.12	0.10	0.09	0.08	0.06
0.6	30	0.12	0.11	0.10	0.09	0.09	0.08	0.07	0.06	0.050
	0	0.13	0.12	0.11	0.10	0.09	0.08	0.07	0.06	0.045
0.7	30	0.08	0.08	0.07	0.07	0.06	0.05	0.05	0.045	0.035
	0	0.09	0.08	0.07	0.06	0.06	0.05	0.05	0.045	0.035
0.8	30	0.05	0.04	0.04	0.04	0.04	0.035	0.03	0.025	0.0235
	0	0.05	0.05	0.04	0.04	0.04	0.035	0.03	0.025	0.0230

Table 2. This table shows the critical semi-major axis  $a_c$  for a planet mass of 30 Jupiter mass, and for a planet of negligible mass, as a function of the mass ratio  $\mu$  and of the eccentricity  $e$  of the binary

The simulations provided a critical semi-major axis, which is where the stable and unstable regions are separated. This means that all semi-major axes below the



critical value are stable and all values that are greater than the critical value are unstable.

## 5 Discussion

Throughout this chapter I will be going through a couple other scientific papers that focused on confirming exoplanets in binary star systems and using that information to learn more about those systems. I will take these examples and compare them back to the previous chapters that I have previously gone through in this thesis.

The first paper “*TIC 172900988: A Transiting Circumbinary Planet Detected in One Sector of TESS Data*,” which was written by lead author Veselin B. Kostov, is about the first confirmation of a circumbinary exoplanet using TESS transit data. Over the course of 5 days the planet was observed to transit both the primary and secondary star. This would mean that this orbit would fit into the P-type classification of exoplanets in binary star systems. TIC 172900988b (the circumbinary exoplanet) has a period of 19.7 days and an eccentricity of 0.45 (Kostov et al. 2021). This is also the only exoplanet that I came across to be confirmed as a P-type exoplanet. Off the bat that opens the door to further discoveries that can help us to grow a deeper understanding of these types of exoplanet orbit, and what may cause them.

The second paper “*Determining Which Binary Component Hosts the TESS Transiting Planet*,” whose lead author is Kathryn V. Lester, takes a survey of potential exoplanets in binary star systems and tries to learn more about them. The data that they pull from is also from the TESS data. Specifically, they were looking

to determine which of the two host stars is hosting these planets, if not both. It's important to determine this for future analysis of the planets, as a lot of the parameters that you can learn about a planet rely on information about the host star. For example, if you are looking at a transit around a star you can create a radius ratio that compares the radius of the planet to the radius of the star. Another great application is that knowing the temperature of the right host star can help us determine if the exoplanet is in the star's habitable zone (Lester et al. 2022).

The results that Lester found say that 70% of their survey orbits around the primary host star, 9% orbits around the secondary host, and 21% orbit around an unknown host (Lester et al. 2022). I believe that the unknown source is likely to just be them orbiting around both hosts, like TIC 172900988b. It's likely that we have yet to observe the transit around the other host. One important detail is that when the secondary host has an apparent magnitude of greater than or equal to 4 mag, the exoplanet is now 89% of the time going to be orbiting the primary host star.

Something that I find especially interesting about all the stars in the two papers is that only one is orbiting both hosts for sure. Based on the theory, I was interpreting that the clearing of the area due to  $a_{crit}$  would make it difficult for planets to orbit only one of the hosts. This would mean that most of the stars, if not all, are forming around both hosts and then moving into the system, as opposed to forming in situ between the planets and then orbiting just one of the two hosts.

Unfortunately, the modeling done by Dr. Capuzzo-Dolcetta only focused on the S-type exoplanets but using what we found in that modeling we may be able to

hypothesize how a P-type exoplanet, such as TIC 172900988b, would act. We would make the same assumptions that they made, that being when an exoplanets orbit leaves the system or collides with one of the stars it is classified as an unstable orbit, otherwise it is classified as a stable orbit. Changing the same parameters, but also adding initial velocity. We would have to add this because it would turn into the same simulation without it. We would then have to use the Gravitational potential that was calculated by Lee and Leung as an updater for the position of the exoplanets. I hypothesize that we would find that the initial position of the exoplanet would be much further out in the system than it is for an S-type exoplanet.

## 6 Conclusion

All in all, we have found out a lot about the existence of exoplanets in binary star systems. Starting back in 2011 when the first exoplanet in a binary star system was confirmed, up to now, we have a solid structure for the equations of state that can describe an orbit of these exoplanets, and well as an understanding of how there is an area that has no dust for exoplanets to form in these systems, because of having two stars. This greatly impacts how we can model and theorize more possibilities within these systems.

Throughout my search I almost entirely came across S-type exoplanets, so the architecture of these types of exoplanets is what I have come to understand the best. In the survey with the 45 different exoplanet candidates, they arrived on the conclusion that the distribution of the orbits can only be explained by a low mutual

inclination between the exoplanets orbit and the plane that the host stars are orbiting. This would lead us to believe that there cannot be a star system with the stars having face on orbits around the central mass, while the planets have edge on orbits around those stars.

Unfortunately, the modeling only dealt with S-type orbits, but that allowed us to discover a critical semi-major axis that determines whether or not an orbit is stable. In the future modeling for both P-type and S-type exoplanets will be a priority, as well as modeling for both in a single system to see how those might interact with each other.

The coolest thing I have learned from this is that we now have an understanding that exoplanets in binary star systems don't innately form less often than exoplanets in single star systems. This means that out in the universe there are probably more Tatooines than there are Earths and isn't that awesome.

## References

- Bromley, B. C., & Kenyon, S. J. (2015). Planet formation around binary stars: Tatooine Made Easy. *The Astrophysical Journal*, 806(1), 98.  
<https://doi.org/10.1088/0004-637x/806/1/98>
- De Cesare, G., & Capuzzo-Dolcetta, R. (2021). On the stability of planetary orbits in binary Star Systems I. The S-type orbits. *Astrophysics and Space Science*, 366(6). <https://doi.org/10.1007/s10509-021-03959-x>
- Kostov, V. B., Powell, B. P., Orosz, J. A., Welsh, W. F., Cochran, W., Collins, K. A., Endl, M., Hellier, C., Latham, D. W., MacQueen, P., Pepper, J., Quarles, B., Sairam, L., Torres, G., Wilson, R. F., Bergeron, S., Boyce, P., Bieryla, A., Buchheim, R., ... Winn, J. N. (2021). TIC 172900988: A transiting

- circumbinary planet detected in one sector of TESS Data. *The Astronomical Journal*, 162(6), 234. <https://doi.org/10.3847/1538-3881/ac223a>
- Lester, K. V., Howell, S. B., Ciardi, D. R., & Matson, R. A. (2022). Determining which binary component hosts the TESS Transiting Planet. *The Astronomical Journal*, 164(2), 56. <https://doi.org/10.3847/1538-3881/ac75ee>
- Dupuy, T. J., Kraus, A. L., Kratter, K. M., Rizzuto, A. C., Mann, A. W., Huber, D., & Ireland, M. J. (2022). Orbital Architectures of planet-hosting binaries – II. low mutual inclinations between planetary and stellar orbits. *Monthly Notices of the Royal Astronomical Society*, 512(1), 648–660. <https://doi.org/10.1093/mnras/stac306>
- Doyle, L. R., Carter, J. A., Fabrycky, D. C., Slawson, R. W., Howell, S. B., Winn, J. N., Orosz, J. A., Prša, A., Welsh, W. F., Quinn, S. N., Latham, D., Torres, G., Buchhave, L. A., Marcy, G. W., Fortney, J. J., Shporer, A., Ford, E. B., Lissauer, J. J., Ragozzine, D., ... Fischer, D. (2011). Kepler-16: A transiting Circumbinary Planet. *Science*, 333(6049), 1602–1606. <https://doi.org/10.1126/science.1210923>